REDESIGNED WITH ALL OF US IN MIND

MERCK

Introducing the Stericup® E and Steritop® E sterile filtration devices—**evolved with an eco-conscience**.

This progressive rethinking of filter design reduces your lab's environmental impact by eliminating the need for a receiver funnel, significantly decreasing packaging and biohazardous waste.

Expect the same faultless filtration you trust from Stericup® devices—and leave a smaller footprint.

Stericup® E family of sterile filters thread directly onto virtually any media bottle

Up to 48% Reduced Plastics

Up to 69% Reduced Packaging

SigmaAldrich.com/Stericup-E

*Up to 48% plastic reduction and 69% packaging reduction (depending on receiver volume), derived from comparison to traditional Stericup® sterile filters.

2019 - 24573 01/2020

The life science business of Merck operates as MilliporeSigma in the U.S. and Canada.

Millipore®

Preparation, Separation, Filtration & Monitoring Products

Received: 1 August 2019 | Revised: 25 October 2019 | Accepted: 22 November 2019

DOI: 10.1002/bit.27233

ARTICLE

BIOTECHNOLOGY BIOENGINEERING WILEY

Continuous ultrafiltration/diafiltration using a 3D-printed two membrane single pass module

Ruijie Tan | Matthias Franzreb

Bioengineering and Biosystem, Institute of Functional Interfaces, Karlsruhe Institute of Technology, Karlsruhe, Germany

Correspondence
Matthias Franzreb, Institute of Functional Interfaces, Karlsruhe Institute of Technology, Eggenstein-Leopoldshafen, Karlsruhe, 76344, Germany.
Email: matthias.franzreb@kit.edu

Abstract

A 3D printed ultrafiltration/diafiltration (UF/DF) module is presented allowing the continuous, simultaneous concentration of retained (bio-)molecules and reduction or exchange of the salt buffer. Differing from the single-pass UF concepts known from the literature, DF operation does not require the application of several steps or units with intermediating dilution. In contrast, the developed module uses two membranes confining the section in which the molecules are concentrated while the sample is passing. Simultaneously to this concentration process, the two membranes allow a perpendicular in and outflow of DF buffer reducing the salt content in this section. The module showed the continuous concentration of a dissolved protein up to a factor of 4.6 while reducing the salt concentration down to 47% of the initial concentration along a flow path length of only 5 cm. Due to single-pass operation the module shows concentration polarization effects reducing the effective permeability of the applied membrane in case of higher concentration factors. However, because of its simple design and the capability to simultaneously run UF and DF processes in a single module, the development could be economically beneficial for small scale UF/DF applications.

KEYWORDS

3D-printing, continuous, SPDF, SPTFF, UFDF

1 | INTRODUCTION

Ultrafiltration (UF) is a powerful membrane technology to separate dissolved macromolecules from low molecular weight components (Zeman & Zydney, 1996). According to their retention properties, UF membranes are especially useful to concentrate dilute product streams in the biotechnological industry. Another common application of UF membranes is within the frame of so-called diafiltration (DF) applied to reduce the ionic strength or change the buffer type in which the retained macromolecules are dissolved (McGregor, 1986). During DF the feed solution buffer is continuously or stepwise diluted by the addition of pure water or a new buffer, while constantly withdrawing a part of the solution as permeate through the UF membrane (Schwartz, 2003). During the process of concentration of the biomolecule solution by UF/DF, the permeate flux declines over time mostly because of concentration polarization near the surface of the membrane and the increasing viscosity of the recirculated feed solution (Shire, 2009). Therefore, the conventional way of operation of the UF/DF system in biotechnology is so-called tangential flow filtration (TFF) in which the fluid flows mainly parallel to the plane of the membrane and at relatively high speed, resulting in the prevention of pronounced concentration polarization and membrane fouling. However, the high flow speed leads to only small concentration effects during one passage through the UF/DF system (Lutz, 2015; van Reis & Zydney, 2007). In consequence, frequent recirculation of the feed solution in a loop is required, strongly increasing the energy demand, and resulting in the danger of unwanted temperature

increase. The high flow speed and frequent recirculation also increases the shear stress onto the dissolved substances and can result in foaming problems, which may lead to damage or denaturation of sensitive biomolecules (van Reis & Zydney, 1999). An alternative to TFF is normal flow filtration (NFF), also called dead-end filtration, in which the flow velocity is perpendicular to the plane of the membrane. NFF prevents high shear stress but quickly leads to strong concentration polarization, membrane plugging, and very low fluxes through the membrane. As a possible solution to this dilemma, single-pass tangential flow filtration (SPTFF) has been developed by Gaston de los Reyes in 2005 (US 7,384,549 B2; De los Reyes and Mir, 2008). Applications of single-pass UF with the tangential flow have been reported before, for example, for blood concentration (Tamari et al., 1983), however, De los Reyes and Mir specially adapted the technology to protein concentration and optimized multimodule setups.

The basic principle of SPTFF is to improve the conversion of a single pass, saying the ratio between the permeate and the feed flow and therefore the concentration factor of the target solute, by increasing the residence time. Increasing the residence time can be accomplished by reducing the feed flow or increasing the flow path length within the membrane module (Casey, Gallos, Alekseev, Ayturk, & Pearl, 2011). Although operating with a single pass of the fluid, compared with dead-end filtration SPTFF still has the advantage of tangential flow having the potential to sweeping away, for example, aggregated molecules from the surface of the membrane and limiting concentration polarization. Additional benefits of SPTFF are the avoidance of additional piping, storage, and control instrumentations for the loop section of conventional TFF (Casey, Rogler, Gjoka, Gantier, & Ayturk, 2018; EMD Millipore, 2014; Lutz, 2015). Original SPTFF was mainly used for debottlenecking downstream processes by concentrating process streams between two unit operations, for example, chromatography steps (Dizon-Maspat, Bourret, D'Agostini, & Li, 2012; Teske & Lebreton, 2010). SPTFF also proved useful for decoupling upstream and downstream process units by the inline concentration of clarified cell culture broth (Arunkumar, Singh, Peck, Borys, & Li, 2017; Brinkmann, Elouafiq, Pieracci, & Westoby, 2018). Recently, SPTFF has been reported as an interesting tool for continuous DF (Jungbauer, 2013; Rucker-Pezzini et al., 2018). In this operation mode, several SPTFF units are sequentially connected while the DF buffer is added between the units. Passing the first SPTFF unit the feed is concentrated by a certain factor, followed by dilution with DF buffer, usually to a level at which the target biomolecule reaches the concentration originally present in the feed. By this, using an arrangement with three modules, Rucker–Pezzini could demonstrate a continuous buffer exchange >99.7% with the help of SPTFF. Regarding the required amount of DF buffer, the efficiency of such an arrangement could even be improved by realizing a counter-current principle, in which fresh DF buffer is only applied in the feed of the last SPTFF stage, while the permeate of this stage is used for dilution of the feed of the preceding SPTFF stage (Nambiar, Li, & Zydney, 2018). Nevertheless, independent of using con-current or counter-current routing of the buffer, continuous DF using SPTFF requires sequential concentration and dilution of the target biomolecule. If the sequence starts with the concentration step in the first SPTFF module, the degree to which this concentration can be done without the risk of forming aggregates or operating at impracticable low permeate fluxes is limited. If the sequence starts by diluting the feed with DF buffer in front of each SPTFF module, the degree of this dilution is limited by the condition that the required buffer amount should be minimized. Up to now, no SPTFF module has been reported, which allows a gentle DF process at constant or slightly increased target molecule concentration, as it is the case in conventional DF with the continuous replacement of the permeate volume by fresh DF buffer.

Therefore, it was the purpose of this study to design and investigate a first small prototype of an SPTFF system realizing continuous, and truly simultaneous UF and DF operation by the use of a two membrane set-up. Applying commercial UF membrane sheets and high-resolution 3D-printing techniques, a device is fabricated in which the feed flows through a narrow channel formed by two adjacent membranes and a porous spacer between. By this, one membrane can operate in SPTFF mode while the second membrane simultaneously is permeated by pure water or DF buffer, gradually replacing the solution in the channel. Controlling the pressures in the different fluid reservoirs of the device as well as the residence time of the feed solution in the central channel, the degree of concentration as well as buffer exchange can be adjusted independently.

2 | MATERIAL AND METHODS

2.1 | Protein solution and membrane

The model protein used for UF/DF experiments was bovine serum albumin (BSA; molar weight 66.5 kDa) purchased from PanReac AppliChem (Darmstadt, Germany). The feed solution was prepared by dissolving BSA powder (0.1 g/l) and sodium chloride (100 mM; Merck KGaA, Darmstadt, Germany) in ultrapure water, the pH of the solution was determined as 6.40. The ultrapure water for buffer preparation was produced by a Sartorius arium® pro system (Sartorius, Göttingen, Germany). For buffer exchange, a low salt solution containing 5 mM of NaCl was used. The used OMEGA ultrafiltration polyethersulfone membrane (30 kDa MWCO, OT030SHEET, Lot. #H3186I) was purchased from Pall Life Sciences (Hauppauge). According to the manufacturer, the water permeability and BSA passage of this membrane are given as 458.5 L/(m^2 h bar) and 0.86%, respectively.

2.2 | 3D printed UF/DF module

All experiments were performed with a self-designed DF module shown in Figure 1. Except for the membrane all parts of the module were 3D printed with a PolyJet system EDEN 260 (Stratasys, Eden Prairie) using the material VeroWhite. VeroWhite is a UV curable polyacrylate polymer with good chemical resistance. The PolyJet technology offers a nominal resolution of 17 µm in the z-direction and around 40 µm in x,y direction, delivering the required resolution for smooth surfaces that

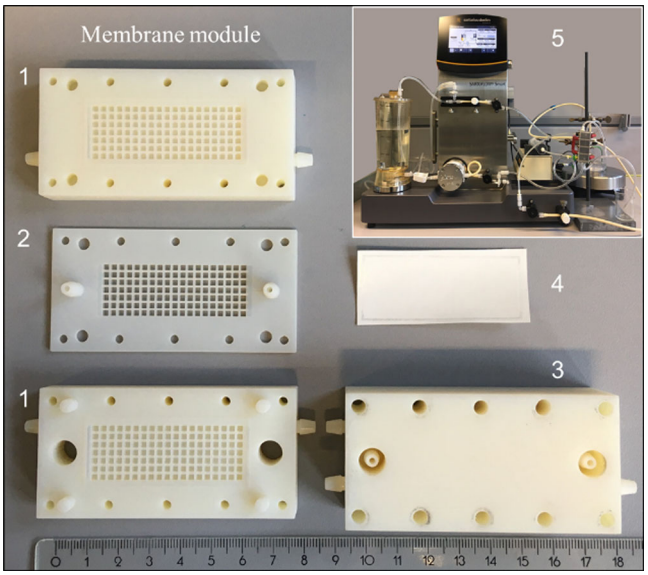

FIGURE 1 3D-printed UF/DF module for single-pass diafiltration: 1. lateral part, 2. middle part, 3. assembled module, 4. commercial OMEGA ultrafiltration membrane, 5. UF/DF peripheral equipment. UF/DF, ultrafiltration/diafiltration [Color figure can be viewed at wileyonlinelibrary.com]

can be sealed by the membrane and the fine channel structures within the module. The PolyJet technology uses a support material to realize the closed channel structure. After the printing, the support material is dissolved by 1 M sodium hydroxide solution overnight.

The 3D-printed membrane module is assembled of three parts, two lateral parts, and one middle part, which form the required liquid distribution system and provide mechanical support for membranes. The module contains two rectangular membrane sheets, one on each side of the middle part. The size and hold up volume of the central section of the middle part are $20 \times 50 \times 2\ mm^3$ and 1.4 ml, respectively. The membrane is supported by a grid-like structure with` 1 mm thick walls at a distance of 3 mm. To allow the tangential flow along the membrane, the walls are perforated by $1 \times 2\ mm^2$ openings. Subtracting the area covered by the printed support grid, an effective membrane area of $0.000532\ m^2$ results on each side. A syringe pump (Pump 11, Harvard Apparatus, Holliston, MA) is used to enter the feed solution into the middle part in a single pass operation mode. Perpendicular to the flow direction of the feed solution, the flow of the exchange buffer is controlled by a conventional lab-scale UF/DF system (SARTOFLOW® Smart, Sartorius). The use of such a conventional UF/DF system is not mandatory for operating the developed module, however, it allowed the automatic recording of the mass changes of the exchange buffer storage and of the permeate.

2.3 | Description of the experimental set-up and the monitored parameters

The described membrane module was integrated into an experimental set-up for UF/DF experiments as shown in the scheme of Figure 2. For simultaneous single pass UF and DF, the feed solution was pumped into the module with a constant volume flow Q_F controlled by a syringe pump. The volume flow Q_R leaving the middle part of the module was controlled by a throttle valve in the outlet and the pressure P_R was monitored by a sensor. The peristaltic pump of the conventional UF/DF system was used to pump the exchange buffer in a loop through the upper part of the module. In the loop, two sensors monitored the pressures $P_{DF,in}$ and $P_{DF,Out}$ at the inlet and the outlet of the upper module part. $P_{DF,in}$ and $P_{DF,out}$ was controlled by a throttle valve located downstream of the $P_{DF,out}$ sensor as well as the adjusted flow in the loop. When the pressures $P_{DF,in}$ and $P_{DF,out}$ in the upper module part were adjusted above the pressure P_R in the middle part, a specific flux J_{DF} of exchange buffer passed the UF membrane "a" between the respective module parts. The exchange buffer storage was placed on a balance allowing accurate monitoring of the volume flow Q_{DF}, which is given by the specific flux J_{DF} times the effective membrane area. The pressure at the lower part of the module was kept at atmospheric pressure, resulting in a pressure difference TMP_P between the middle part and the lower part and a corresponding specific flux Jp through the second membrane "b". The resulting permeate volume flow Q_P could leave the lower module part via two outlets and be collected in a small beaker placed on a second balance. In summary, the operation of the developed system could be accurately monitored and described by six parameters, the volume flows Q_{DF}, Q_P, Q_F, and Q_R as well as the transmembrane pressures TMP_{DF} and TMP_P. Q_F, TMP_{DF}, and TMP_P were given or known from the applied pressure sensors; Q_{DF}, Q_P, and Q_R were calculated from the time-resolved monitoring of the respective masses m_{DF}, m_P, and m_R.

2.4 | Experimental procedure

Experiments were performed by first adjusting the constant feed volume flow Q_F as 0.5 ml/min by the help of the syringe pump and the volume flow in the loop by the help of the peristaltic pump of the conventional UF/DF system. Afterward pressure valves downstream of the sensors $P_{DF,out}$ and P_R were regulated to set Q_R and the transmembrane pressures TMP_{DF} and TMP_P. Because of the interplay of these parameters, their control required some

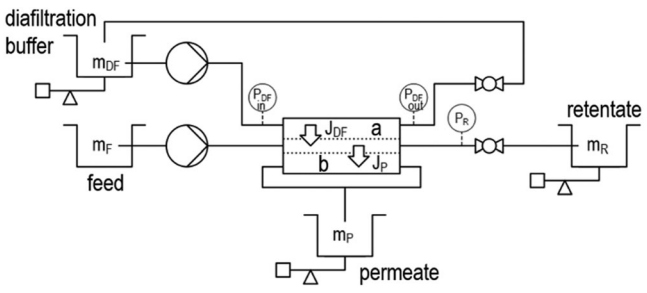

FIGURE 2 Scheme of the flow paths and different control points of the developed two-membrane module for simultaneous ultra- and diafiltration

experience and several readjustments. After the parameters settled at the desired values, the system was operated for at least another 30 min to guarantee steady-state conditions. To check if the dependencies between transmembrane pressures and resulting fluxes follow the rules known from conventional UF/DF systems, the water fluxes passing membranes "a" and "b" were determined for different operation conditions. Nine sets of parameter conditions were chosen with TMP_{DF} and TMP_P in a range of 0.07–0.3 bar. After adjusting a new parameter set and reaching a steady-state, the volume flows Q_R, Q_{DF}, and Q_P were determined by averaging over a period of 10 min.

After characterizing the hydrodynamic behavior of the system, a series of experiments with a feed solution containing BSA and NaCl were conducted. The execution of the experiments mainly followed the procedure described in the section above. However, in case of low volume flows Q_R it turned out to be difficult to reliably achieve constant volume flows with the help of the simple throttle valve available. Therefore, another way of controlling the average volume flow Q_R was chosen by completely closing the respective valve for an interval of 2, 4, 6, and 12 min, respectively, and opening and releasing a defined amount of liquid only in short defined intervals in between. Although this operation mode is not fully continuous anymore, it has the advantage of easy control and reliable adjustment of the average flow. In addition to the measurement of the exchange buffer and permeate masses, BSA concentration and conductivity were measured in the collected retentate samples. The concentration of BSA was measured by UV spectroscopy (PerkinElmer Enspire®) based on the absorbance at 280 nm. Conductivity was measured by a conductometer (WTW LF330; Weilheim, Germany) equipped with cell (WTW TetraCon® 325, Weilheim, Germany). In the investigated concentration range the contribution of the concentration of BSA on the conductivity can be neglected, and in good approximation, the conductivity is directly proportional to the concentration of NaCl as $c_{NaCl,R} = c_{NaCl,F} \times \frac{\lambda_R}{\lambda_F}$, with λ_F, λ_R being the conductivity of the feed and retentate, respectively. In our experiments, the feed solution having a concentration of NaCl of 100 mM was partly exchanged by DF buffer (5 mM NaCl) during the single pass through the filtration module. Therefore, the degree of buffer exchange can be calculated from the conductivities by

$$\text{Buffer exchange (\%)} = \frac{\lambda_F - \lambda_R}{\lambda_F - \lambda_{DF}} \times 100\%, \quad (1)$$

with λ_{DF} being the conductivity of the DF buffer.

3 | RESULTS AND DISCUSSION

3.1 | Water fluxes and protein concentration-dependent permeability

As described, a commercial membrane was used in all experiments of this study. To ensure the validity of water permeability data given by the manufacturer also in the unusual set-up with three pressure levels and membrane "a" operating in a crossflow manner while membrane "b" operating under single pass conditions, the resulting fluxes of pure water were measured for the expected parameter range. Figure 3 shows that the water fluxes of the membranes "a" and "b" increased linearly with the corresponding TMP. From the slope of the linear fit the permeabilities of membrane "a" and membrane "b" were found to be 487.9 ± 8.0 L/(m^2 h bar) (R^2 = 0.998) and 442.5 ± 8.2 L/(m^2 h bar) (R^2 = 0.997), respectively. Therefore, the permeabilities are equal within an experimental error of less than 10% and closely similar to the value given by the manufacturer 459 (L/m^2 h bar).

SPTFF applies much slower flow velocities within the membrane filtration modules than conventional TFF, which pumps the retentate in a loop. Therefore, the ability to prevent concentration polarization in front of the UF membrane is reduced. In the case of our module design which uses an additional perpendicular flow of DF buffer within the module for simultaneous UF and DF, this problem is even enhanced, because the flux through membrane b is formed by the sum of the permeate and the DF fluxes. Therefore, additional experiments have been conducted studying the dependency of

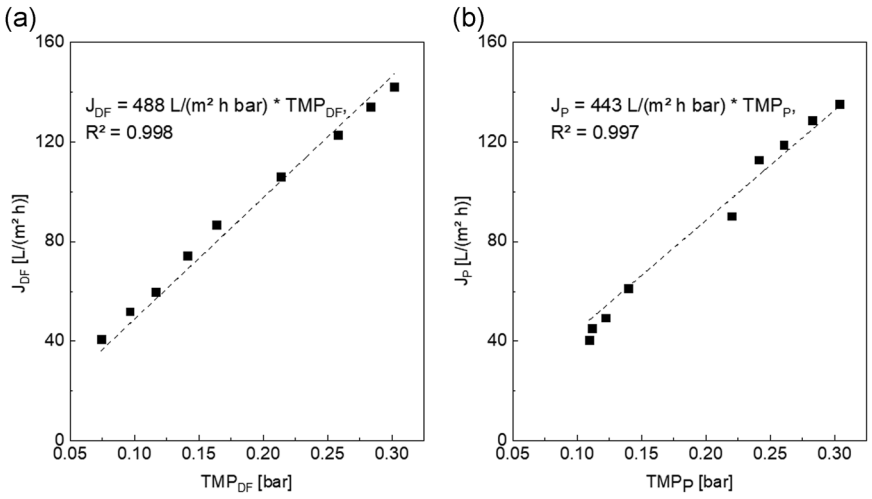

FIGURE 3 Water flux of membranes 'a' and "b" in the module calculated by mass balances of experiments with different volume flows Q_F and Q_R and different transmembrane pressures TMP_{DF} and TMP_P. (a) membrane 'a'; (b) membrane 'b'

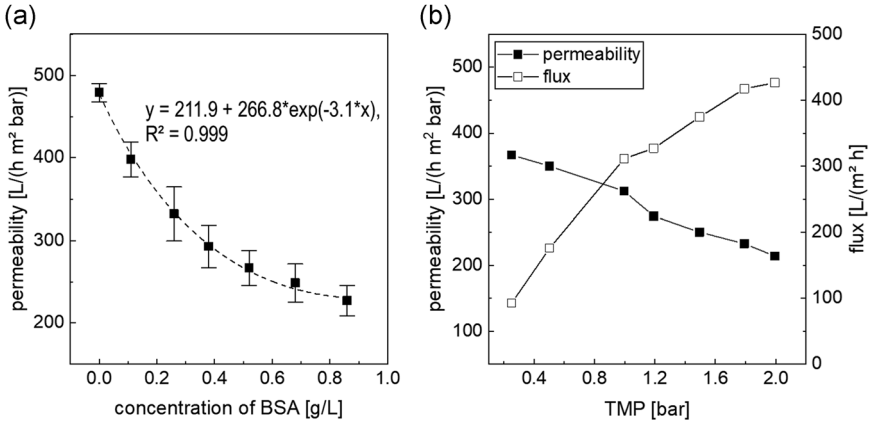

FIGURE 4 Membrane permeability in dependence of BSA concentration and applied transmembrane pressure. The experiments were conducted in conventional TFF mode using only one membrane. This was achieved by removing the middle part of the module and returning the retentate to the feed tank in a loop. (a) Variation of BSA concentration in the retentate loop. The initial BSA concentration in the loop was 0.1 g/L BSA in 100 mM NaCl, except for the first point, which shows the permeability in case of pure water. Afterward, the BSA concentration was increased stepwise by adding increasing volumes of a concentrated BSA stock solution to the loop. The applied transmembrane pressure was constant at 0.75 bar except for the experiment applying pure water (TMP = 0.3 bar). (b) Effect of TMP onto permeability and flux of the used UF membrane, feed solution 0.1 g/L BSA, 100 mM NaCl. BSA, bovine serum albumin

membrane permeability on the BSA concentration in the retentate and the applied transmembrane pressure. Figure 4a shows the decrease of the permeability of membrane "b" with increasing BSA concentration. The permeability follows the expected trend with an approximately exponential decrease with increasing BSA concentration, however, compared with conventional TFF the decrease is strongly pronounced even at rather low protein concentrations. On the other hand, the decrease seems to level off at a permeability of around 200 L/(h m^2 bar) in case of BSA concentrations of around one gram per liter. Therefore, the SPTFF with combined UF and DF seems to be suitable for low to moderately concentrated protein solutions. In the second series of experiments we investigated to which extent the increase of the transmembrane pressure increases the flux and if an optimal operation point could be identified. Figure 4b shows that within the examined range the flux steadily rises with increasing transmembrane pressure, however, in a nonlinear fashion. The flux curve shows no clear transition point but rather a constantly decreasing slope, which also indicates in an almost linear decrease of the permeability with increasing transmembrane pressure. Therefore, no clear optimum could be identified and the achievable performance seems to be limited by the pressure resistance of the UF membrane and the 3D-printed SPTFF module.

3.2 | Time course of the UF/DF experiments

In the following, the time required to reach stationary UF/DF operation conditions has been investigated. For this, experiments with a feed solution containing 0.1 g/l BSA and 100 mM NaCl at a constant feed flow Q_F = 0.50 ml/min was conducted and samples of the effluent Q_R were taken in intervals of 5 or 10 min. Because the module was filled with ultrapure water initially, the course of the effluent concentrations of both substances starts at zero and approaches a constant plateau after reaching stationary conditions. Figure 5a shows the time courses of the effluent concentrations of BSA and NaCl in case of an experiment having its focus only on DF ($c_{BSA,R}/c_{BSA,F} \approx 1$). As can be seen, BSA and NaCl reach their plateau after around 40 min. The experiments were conducted in triplicates and the resulting standard deviations indicate that the module performance and its start-up behavior are highly reproducible. According to the records of the weight differences Δm_R, Δm_{DF}, and Δm_P determined for every interval, the average volume flows in the membrane module were calculated to be Q_R = 0.42 ml/min, Q_{DF} = 0.50 ml/min, and Q_P = 0.58 ml/min. Together with the applied feed flow of Q_F = 0.50 ml/min the mass balance closes completely if a constant solution density is assumed. A residence time (RT) of the solution of around 3.3 min in the middle grid can be calculated by the division of the free volume of the middle module part (1.4 ml) and the average retentate flow Q_R. Considering the volume of the tubing before and after the module (3 and 4 ml), the total residence time increases to 19.5 min. Comparing the residence time and the duration of 50 min to reach stationary conditions, it shows that it requires around two times the residence time to reach a stationary state. This ratio indicates a relatively strong mixing within the middle part of the module, which we think is mainly due to the grid structure and the short length of only 5 cm of the flow path. In this experiment a reduction of the salt concentration down to 52.3% of the inlet concentration was observed, while the ratio between the BSA concentration in the outlet and the one in the inlet approached the expected value of 1.2, indicating that the module was operated in plain DF mode.

In case of ideal DF behavior with constant transversal plug flow between the feed inlet and retentate outlet ($Q_R = Q_F$ and therefore also $Q_{DF} = Q_P$) the salt concentration in the retentate can be calculated by (the derivation of this equation is given in the SI part)

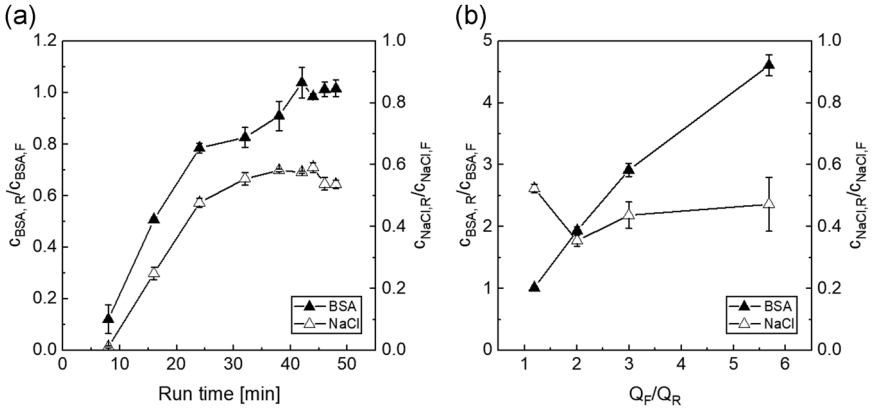

FIGURE 5 (a) Time course of bovine serum albumin (BSA) and NaCl concentration in the retentate for an experiment with Q_F/Q_R = 1.19, Q_P/Q_{DF} = 1.16, TMP_P/TMP_{DF} = 2.07, (b) effect of the volume flow ratio Q_F/Q_R onto the achieved concentration factor of BSA and the resulting reduction of the salt concentration after achieving stationary conditions. Q_F/Q_R = 1.19; 2.01; 3.00; 5.68, Q_{DF}/Q_P = 0.86; 0.88; 0.63; 0.57, TMP_P/TMP_{DF} = 2.07, 4.16; 6.21; 5.04, respectively. Error bars are equal to ± standard deviation

$$c_{NaCl,R} = \left(c_{NaCl,F} - c_{NaCl,DF}\right) \times \exp\left(-\frac{Q_P}{Q_F}\right) + c_{NaCl,DF}. \quad (2)$$

If the salt concentration in the DF buffer is zero ($c_{NaCl,DF} = 0$) Equation (2) reduces to a form which is similar to the well-known equation of constant volume DF in a conventional TFF system (Lutz, 2015), however, with the volumes of the initial feed and the used DF buffer replaced by the respective volume flows. Equation (2) gives a predicted value of $c_{NaCl,R}/c_{NaCl,F}$ = 35%, which is only two third of the experimental value of 52.3%. In fact, the experimental value is much closer to the predicted value, if ideal mixing is assumed within the retentate chamber (see Table 1). In this case, the local salt concentration in the permeate is constant throughout the module and equals the salt concentration in the retentate. Solving the respective mass balance

$$\begin{aligned} c_{NaCl,R} &= \left(c_{NaCl,F} \times Q_F + c_{NaCl,DF} \times Q_{DF}\right)/(Q_P + Q_R) \\ &= \left(c_{NaCl,F} \times Q_F + c_{NaCl,DF} \times Q_{DF}\right)/(Q_F + Q_{DF}). \end{aligned} \quad (3)$$

results in a predicted value of $c_{NaCl,R}/c_{NaCl,F}$ = 52.7%. The good agreement is a clear indication of the backmixing within the short module, corresponding with a reduced DF efficiency.

3.3 | Concentration and DF with varying volume flow ratios

Finally, a series of experiments was conducted aiming to achieve substantial concentration factors of BSA while simultaneously reducing the salt content and operating in a continuous fashion. Figure 5b shows the expected behavior with the concentration factor of BSA increasing almost linearly with increasing volume flow ratio Q_F/Q_R

$$\frac{C_{BSA,R}}{C_{BSA,F}} = \frac{Q_F}{Q_R} \quad (4)$$

The only exception from the ideal relationship was observed in the case of repeated experiments with a Q_F/Q_R ratio above five. In these experiments, the concentration factor stayed about 20% below the expectations, assumingly because of the nonideal BSA retention of the membrane and some BSA accumulation within the module. The influence of this nonideality starts to grow with increasing concentration and increasing residence time, as it is the case for decreasing retentate flows Q_R while the feed flow Q_F is kept at 0.5 ml/min. Keeping the feed flow Q_F at a constant value and reducing the retentate flow Q_R, it could expect a slight decrease of

TABLE 1 Comparison of the measured salt reduction efficiencies with the predictions of the two idealized theoretical models, (i) plug flow and (ii) complete mixing of feed and diafiltration buffer in the module

Flow rate ratio Q_F/Q_R (−)	Experimental result, $C_{R,\ NaCl}$ (mM)	Plug flow[(i)], $c_{R,\ NaCl}$ (mM)	Complete mixing[(ii)], $c_{R,\ NaCl}$ (mM)	Q_{DF} (ml/min)	Q_P (ml/min)
2	52.3	35.0	52.7	0.5	0.6
4	35.5	20.8	41.7	0.8	0.9
6	43.7	27.7	56.2	0.5	0.7
12	47.2	32.1	60.5	0.3	0.6

(i) $c_R = (c_F - c_{DF}) \times \exp\left(-\frac{Q_P}{Q_F}\right) + c_{DF}$

(ii) $c_R = \frac{Q_F \times c_F + Q_{DF} \times c_{DF}}{Q_F + Q_{DF}}$

the remaining salt content in the retentate if the flow of the DF buffer through membrane "a" Q_{DF} would stay at a constant level. Because of conservation of mass, in this case, Q_P would have to increase for decreasing retentate flow, and with increasing Q_P a higher amount of salt would be transferred into the permeate. However, in reality, our experiments showed a decrease in the volume flow Q_{DF} with increasing volume flow ratio Q_F/Q_R and a corresponding slight decrease of Q_P. Nevertheless, the experiments show that the developed module allows setting the levels of protein concentration by UF and salt removal by DF independently, by adjusting the input flows and pressures in the module parts. At a given feed flux per membrane area of 56 L/(m^2 h) our system reached a concentration factor (CF) of 4.5, which compares well with the SPTFF concentration factors reported in literature in case of comparable feed fluxes (CF 3–4 in case of a feed flux of 52 L/(m^2 hr) (Dizon-Maspat et al., 2012), and CF 5 in case of a feed flux of 55 L/(m^2 hr) (Arunkumar et al., 2017)). As can be seen from Table 1, the achieved salt concentrations were in a range between 35% and 52% of the salt concentration in the feed. This degree of salt reduction will be too low for most practical applications requiring DF, however, one has to take into account that the salt reduction is achieved using a very short flow path length in the SPTFF module of only 5 cm. Comparing the experimental results with the predictions of the two idealized SPTFF models introduced in Section 3.2 one finds that the measured retentate salt concentrations are in-between. Therefore, the flow regime within the SPTFF module seems to be in-between complete mixing and plug flow, with a tendency to complete mixing at low CF values, corresponding with shorter residence times within the module. Nevertheless, increasing the flow path length to for example, 50 cm while keeping the width constant, the middle part of the module resembles a long narrow channel with permeable walls and it can be expected, that the flow regime approaches plug flow conditions more and more. Using Equation (2) and the assumption of a constant flux of DF buffer through membrane "a" per length of the flow path it can be estimated that a single 50 cm SPTFF module of our design should be able to reach DF efficiencies beyond 99%.

4 | CONCLUSION AND OUTLOOK

The data presented show that the developed 3D-printed UF/DF is able to concentrate large biomolecules, for example, proteins, of a continuous sample feed while simultaneously reducing the salt amount of the sample matrix. This is achieved by the application of two membranes allowing the continuous in- and outflow of pure water or DF buffer perpendicular to the flow direction of the sample stream. This feature clearly differs our set-up from other single-pass TFF systems, using only one membrane to split the feed into a permeate and a retentate stream. To achieve continuous DF with such systems, several units have to be assembled in a row with dilution in between. In our system, the degree of simultaneous DF and UF can be chosen independently by adjusting the pressures in the upper and middle parts of the module, as well as the volume flow ratio between the sample feed and the outlet of the middle part of the module. We are aware that the demonstrated degree of around 55% buffer exchange is much lower than the values of 99 or even 99.9% often requested in biopharmaceutical downstream processes, and that 55% buffer exchange would be easily achievable in a single unit of the known SPTFF systems. However, to reach 99% or 99.9% buffer exchange in a single unit of a conventional SPTFF the initial dilution would have to be 100 or even 1,000 times, leading to uneconomical amounts of DF buffer and membrane areas required. Therefore, the process has to be divided into several SPTFF units with an intermediate addition of DF buffer. In contrast, the developed SPTFF module allows a continuous infiltration of DF buffer throughout the complete flow path. Therefore, future modules having a longer flow path should be able to achieve high degrees of buffer exchange within a single SPTFF unit. In the described setup the flow and the pressure in the upper part of the module are controlled by a conventional UF/DF system. However, optimized future versions of the set-up could use simple pressure-controlled reservoirs for controlled delivery of the DF buffer to the upper part of the module. In addition, besides the described simultaneous UF/DF mode, the module could also be used for plain single-pass TFF operation if required. In this case the direction of the flux passing membrane "a" would be reversed by adjusting $P_{DF,in}$ and $P_{DF,out}$ to ambient pressure. By this, the membranes on both sides of the retentate channel will available for UF, as it is the case in conventional TFF and SPTFF modules. Finally, stacked versions of multiple 3D-printed cassettes separated by membranes could be realized, with alternating function as buffer delivery, sample concentration, and salt removal sections. Still, we doubt that the simple planar design of the setup is suitable for high-throughput applications. Rather, the direction of future developments will be further size reduction, parallelization and simplified hydraulics of the setup to allow simple buffer exchange and concentration in the area of bioanalytic and high throughput process development.

ACKNOWLEDGMENTS

R.Tan is supported by the China Scholarship Council. The funding agencies had no influence on the conduct of this research work.

ORCID

Ruijie Tan http://orcid.org/0000-0002-1899-3675
Matthias Franzreb http://orcid.org/0000-0003-3586-4215

REFERENCES

Arunkumar, A., Singh, N., Peck, M., Borys, M. C., & Li, Z. J. (2017). Investigation of single-pass tangential flow filtration (SPTFF) as an inline concentration step for cell culture harvest. *Journal of*

Membrane Science, *524*, 20–32. https://doi.org/10.1016/j.memsci.2016.11.007

Brinkmann, A., Elouafiq, S., Pieracci, J., & Westoby, M. (2018). Leveraging single-pass tangential flow filtration to enable decoupling of upstream and downstream monoclonal antibody processing. *Biotechnology Progress*, *34*(2), 405–411. https://doi.org/10.1002/btpr.2601

Casey, C., Gallos, T., Alekseev, Y., Ayturk, E., & Pearl, S. (2011). Protein concentration with single-pass tangential flow filtration (SPTFF). *Journal of Membrane Science*, *384*(1–2), 82–88. https://doi.org/10.1016/j.memsci.2011.09.004

Casey, C., Rogler, K., Gjoka, X., Gantier, R., & Ayturk, E. (2018). *Cadence™ single-pass TFF coupled with chromatography steps enables continuous bioprocessing while reducing processing times and volumes*. Pall Scientific and Technical Report, Retrieved from http://www.pall.de/pdfs/Biopharmaceuticals/USD3003_Cadence_SPTFF_ChromSteps_AN.pdf

Dizon-Maspat, J., Bourret, J., D'Agostini, A., & Li, F. (2012). Single pass tangential flow filtration to debottleneck downstream processing for therapeutic antibody production. *Biotechnology and Bioengineering*, *109*(4), 962–970. https://doi.org/10.1002/bit.24377

EMD Millipore. (2014). Single-pass tangential flow filtration, (C), 1–4. Retrieved from https://www.emdmillipore.com/Web-CA-Site/en_CA/-/CAD/ShowDocument-Pronet?id=201501.131

Jungbauer, A. (2013). Continuous downstream processing of biopharmaceuticals. *Trends in Biotechnology*, *31*(8), 479–492. https://doi.org/10.1016/j.tibtech.2013.05.011

De los Reyes, G., & Mir, L. (2008). *US Patent No. 7,384,549 B2*.

Lutz, H. (2015). *Ultrafiltration for bioprocessing*. Cambridge: Woodhead Publishing.

McGregor, W. C. (Ed.). (1986). *Membrane separations in biotechnology*. New York: Marcel Dekker Inc.

Nambiar, A. M. K., Li, Y., & Zydney, A. L. (2018). Countercurrent staged diafiltration for formulation of high value proteins. *Biotechnology and Bioengineering*, *115*(1), 139–144. https://doi.org/10.1002/bit.26441

van Reis, R., & Zydney, A. (2007). Bioprocess membrane technology. *Journal of Membrane Science*, *297*(1–2), 16–50. https://doi.org/10.1016/j.memsci.2007.02.045

van Reis, R., & Zydney, A. L. (1999). Protein ultrafiltration. In Flickinger, M. C. & Drew, S. W. *Encyclopedia of bioprocess technology: Fermentation, biocatalysis, and bioseparation* (pp. 2197–2214). New Jersey: John Whiley & Sons, Inc.

Rucker-Pezzini, J., Arnold, L., Hill-Byrne, K., Sharp, T., Avazhanskiy, M., & Forespring, C. (2018). Single pass diafiltration integrated into a fully continuous mAb purification process. *Biotechnology and Bioengineering*, *115*(8), 1949–1957. https://doi.org/10.1002/bit.26708

Schwartz, Larry (2003). Diafiltration for desalting or buffer exchange. *BioProcess International*, *5*, 43–47. Retrieved from. http://www.bioprocessintl.com/multimedia/archive/00077/0105ar06_77637a.pdf

Shire, S. J. (2009). Formulation and manufacturability of biologics. *Current Opinion in Biotechnology*, *20*(6), 708–714. https://doi.org/10.1016/j.copbio.2009.10.006

Tamari, Y., Nelson, R., Levy, R., Rea, N., Salogub, M., Carolina, C., … Tortolani, A. (1983). Conversion of dilute pump blood to whole blood by single pass ultrafiltration. *Journal of ExtraCorporeal Technology*, *15*(5), 126–132.

Teske, C. A., & Lebreton, B. (2010). Inline ultrafiltration. *Biotechnology Progress*, *26*(4), 1068–1072. https://doi.org/10.1002/btpr.404

Zeman, L. J., & Zydney, A. L. (1996). *Microfiltration and ultrafiltration: Principles and applications*. New York: Marcel Dekker Inc.

SUPPORTING INFORMATION

Additional supporting information may be found online in the Supporting Information section.

How to cite this article: Tan R, Franzreb M. Continuous ultrafiltration/diafiltration using a 3D-printed two membrane single pass module. *Biotechnology and Bioengineering*. 2020; 117:654–661. https://doi.org/10.1002/bit.27233